Macromolecules
ARTICLE

*Macromolecules* **2010**, *43*, 249–261 **249**
DOI: 10.1021/ma901830b

# Photochromic Polymer Conjugates: The Importance of Macromolecular Architecture in Controlling Switching Speed within a Polymer Matrix

**Francesca Ercole,[†,‡,§] Nino Malic,[†,‡] Simon Harrisson,[†,‡] Thomas P. Davis,[§] and Richard A. Evans*[,†,‡,§]**

[†]*CSIRO Molecular & Health Technologies, Bag 10, Clayton VIC 3169, Australia,* [‡]*The Cooperative Research Centre for Polymers, 8 Redwood Drive, Notting Hill, VIC 3168, Australia, and* [§]*Centre for Advanced Macromolecular Design, School of Chemical Sciences and Engineering, The University of New South Wales, Sydney, NSW 2052, Australia*

*Received August 17, 2009; Revised Manuscript Received September 28, 2009*

ABSTRACT: Naphthopyran−poly(*n*-butyl acrylate) conjugates with different geometries were assembled using ATRP. First, within a rigid lens matrix, an investigation of the photochromic behavior of various poly(*n*-butyl acrylate), p(*n*-BA), homopolymers showed that midplacement of a single dye moiety, made possible using a Y-branching difunctional photochromic initiator, gave superior fade kinetics per chain length of conjugated polymer compared to end-functionalized homopolymers. Furthermore, having the dye pendant from the chain opposed to directly within the chain was also found to be advantageous. Fading kinetics became faster when chain length was increased, except in the case of linear random copolymers made by copolymerization of *n*-butyl acrylate with a naphthopyran acrylate. A gradient copolymer made with a nonphotochromic difunctional initiator and a naphthopyran methacrylate displayed superior kinetics. Films consisting of ABA triblock copolymers, incorporating the photochromic in the middle of a soft p(*n*-BA) section, gave slower switching speeds compared to lens samples, with responses that were highly tunable and dependent on the amount of soft section inhabited by the photochromic moiety.

## Introduction

Photochromic dyes are well-known for their commercial application in light-sensitive ophthalmic lenses due to their ability to undergo a reversible color change when irradiated with ultraviolet (UV) light.[1] Naphthopyran dyes, also known as chromenes,[2] are noteworthy examples, being able to thermally decolorize in the absence of irradiation, to develop a broad range of intense colors depending on their electronic substitution and to withstand fatigue on prolonged exposure to light.

The photocoloring process takes place via the heterolytic cleavage of the C−O bond in the pyran moiety, resulting in a distribution of isomeric open forms (merocyanines) which are colored due to their extended conjugation and quasi-planar structures. In order to convert from a closed form to an open form, or the reverse, the molecules must undergo a large intramolecular rotation to become coplanar-like in their colored (open) form or orthogonal in their clear (closed) forms (Figure 1).[3,4]

Practical application in ophthalmic eyewear requires that the photochromic compounds be incorporated into the polymer host/substrate using one of several strategies: the process of imbibing integrates the molecules within the top layers of the host;[5] casting-in can be carried out by dissolution or dispersion of the dyes into the host monomers prior to curing the material; or a separate layer of the dyes can be incorporated as a film on top of, in between, or in adjacent layers of the host.[6] However, when photochromic molecules are incorporated into a polymer matrix, their switching speed is found to be considerably slower compared to what can be achieved in solution. This is because within the limited free volume of the plastic host the molecules are restricted in their movement, known as the matrix effect.[7] In an attempt to overcome this drawback, industry has focused on the bulk host material by using plasticizers, by improving the method of dye application, and by developing faster dyes. However, for applications such as spectacles, where hardness and abrasion resistance are important, the components and properties of the substrate cannot be compromised in order to achieve a desired improvement in the rate of coloration and fade.

The control of photochromic switching speed in a rigid host can now be achieved using engineered photochromic−polymer conjugates.[8] This approach has been developed by us using a cast-in method, where an optimized host matrix is left unmodified in order to bring about changes to photochromic performance. Instead, the dye that is added to the host matrix composition has a polymer/oligomer bound directly to it in order to bring about critical changes to its local environment, i.e., what immediately surrounds the dye within the host matrix. A local fluid environment can be introduced around the dye by conjugation to a soft oligomer, such as p(*n*-BA), allowing greater freedom of movement during molecular rotation which results in faster switching.[9]

Specialized dye−polymer conjugates can be constructed using controlled radical polymerization techniques, such as atom transfer radical polymerization (ATRP). This is mainly carried out with the approach of growing well-defined polymers (with controlled molecular weights, $M_n$, and polydispersity indexes, PDI) from photochromic inititiators.[10−13] An important feature of the technology is that tuning of the fade speed of the photochromic material can be achieved by adjusting both the $T_g$ of the polymer and the chain length of the tail. It has recently been demonstrated that the geometry of the conjugate can also affect performance. Larger and more tunable improvements have been observed for the midplacement of the dye within p(*n*-BA),

*Corresponding author. E-mail: richard.evans@csiro.au.



Published on Web 11/02/2009

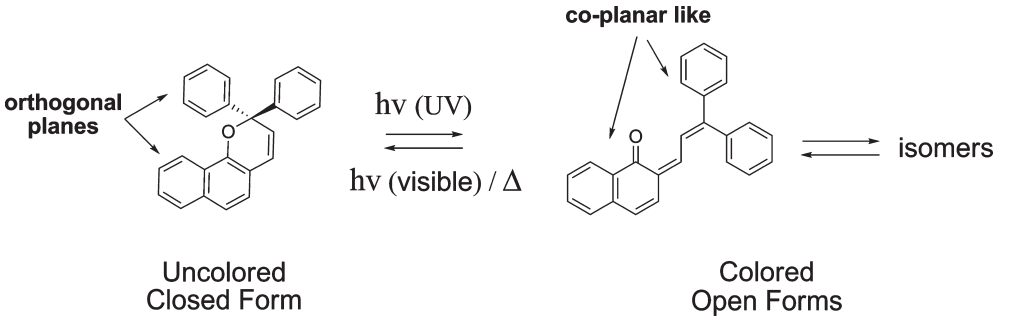


**Figure 1.** Photochromic transition between clear (closed) and colored (open) forms of a 2*H*-naphthopyrans.

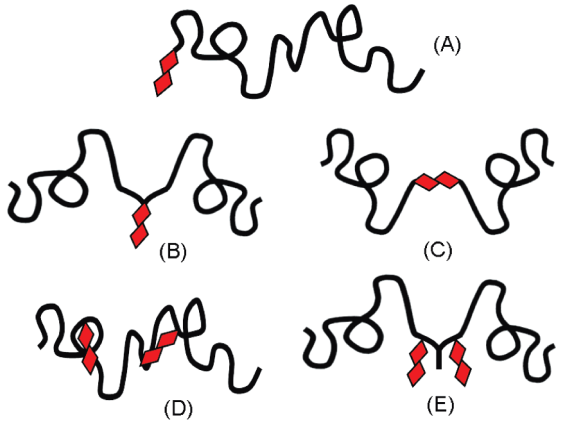


**Figure 2.** Photochromic dye−p(*n*-BA) conjugate strategies: (A) end-placement of the dye; (B, C) midplacement of the dye; (D) random copolymer; and (E) gradient copolymer with pendant photochromic groups, made with photochromic acrylate and methacrylate.

a low-$T_g$ polymer, vs the end placement of a dye.[14,15] This Y-branching approach was developed using an aromatic central scaffold which allows the dye to be attached centrally, and then initiator sights located on opposite sides of the aromatic ring allow the radial growth of two polymer arms.

We believe that chain architecture has an important role in determining the level of encapsulation that can be provided by polymer conjugation and its ability to affect the local environment around the photochromic. The present paper extends this concept by comparing several motifs for applying p(*n*-BA) conjugation to a naphthopyran photochromic, as depicted in Figure 2. End-functional photochromic−polymer conjugates (A) were assembled using a monofunctional photochromic initiator. Midfunctional photochromic−polymer conjugates (B) and (C) were explored using difunctional photochromic initiators. In the case of (B) this was approached using a symmetrical, difunctional initiator which incorporated an aliphatic scaffold, and with (C), two arms were grown biradially from opposite sides of a central photochromic molecule. Photochromic functional monomers were used for the synthesis of random copolymers (D) and gradient copolymer (E), containing pendant dye moieties. ATRP was used to polymerize these structures. Their photochromic performances were then evaluated with reference to one another and to those of unconjugated controls when cast within a rigid host matrix.

Lastly, given the promising results obtained for Y-branching approaches (B) and (E), these p(*n*-BA) structures were extended to make ABA-type triblock copolymers with isobornyl acrylate (IBA), where the photochromic moiety resides within the soft p(*n*-BA) central portion. These block copolymers were made into films and their photochromic behavior was compared to one another and to those of dye-p(*n*-BA) conjugates that were cast in the rigid host matrix.

**Scheme 1. Synthesis of Photochromic Control Compounds 2 and 4**

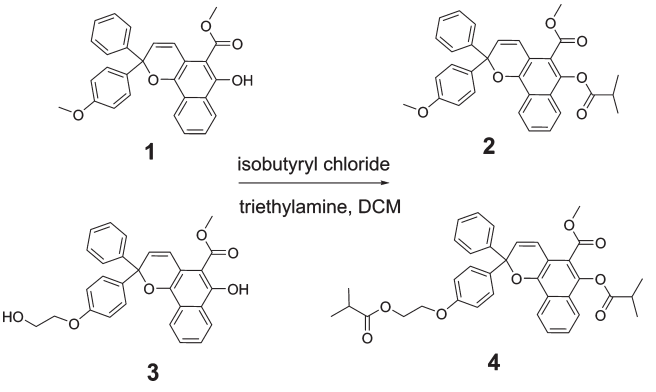


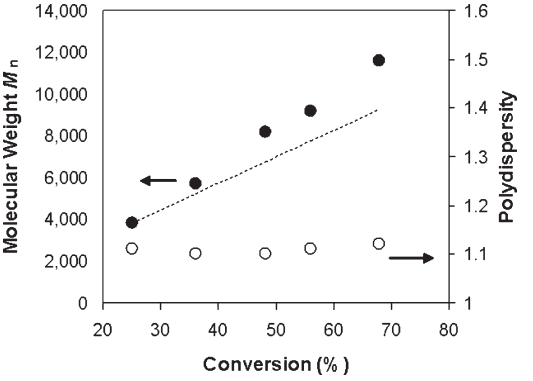


**Figure 3.** Evolution of polydispersity (○) and molecular weight (●) with conversion for the atom transfer radical polymerization of *n*-butyl acrylate with initiator **5** at 90 °C in benzene where [monomer]/[CuBr]/[4,4′-dinonyl-2,2′-bipyridine]/[**5**] = 100:1:2:1. Calculated molecular weight (---) by NMR conversion using the equation $M_n$ = ((monomer MW) × ([monomer]/[**5**]) × (NMR conversion)) + (MW of **5**). Polymerization times ranged from 2 to 12.8 h.

## Results and Discussion

Hydroxy-functional naphthopyrans **1** and **3**[16] were synthesized in high yield, as described in previous publications,[10,14,17] and then converted to the red-coloring isobutyrate derivatives **2** and **4** via simple esterification routes as shown in Scheme 1. With the aim of scrutinizing the effect of polymer conjugation on the performance of the dye, these electronically equivalent controls served as reference points for our tests.

Photochromic ATRP initiators **5** and **7** were also prepared by esterification of these hydroxy-functionalized precursors with 2-bromoisobutyryl bromide (Scheme 2). In the case of photochromic initiator **6**, the aliphatic branching agent, 2,2-bis(hydroxymethyl)propionic acid,[18] was first converted to 2,2-bis(2-bromo-2-methylpropanoyloxymethyl)propanoic acid,[19−21]

**Scheme 2. Atom Transfer Radical Polymerization Synthesis of Naphthopyran−Poly(*n*-butyl acrylate) Conjugates Displaying Molecular Weights of Purified Samples Tested in Survey (dNbpy = 4,4′-Dinonyl-2,2′-bipyridine)**

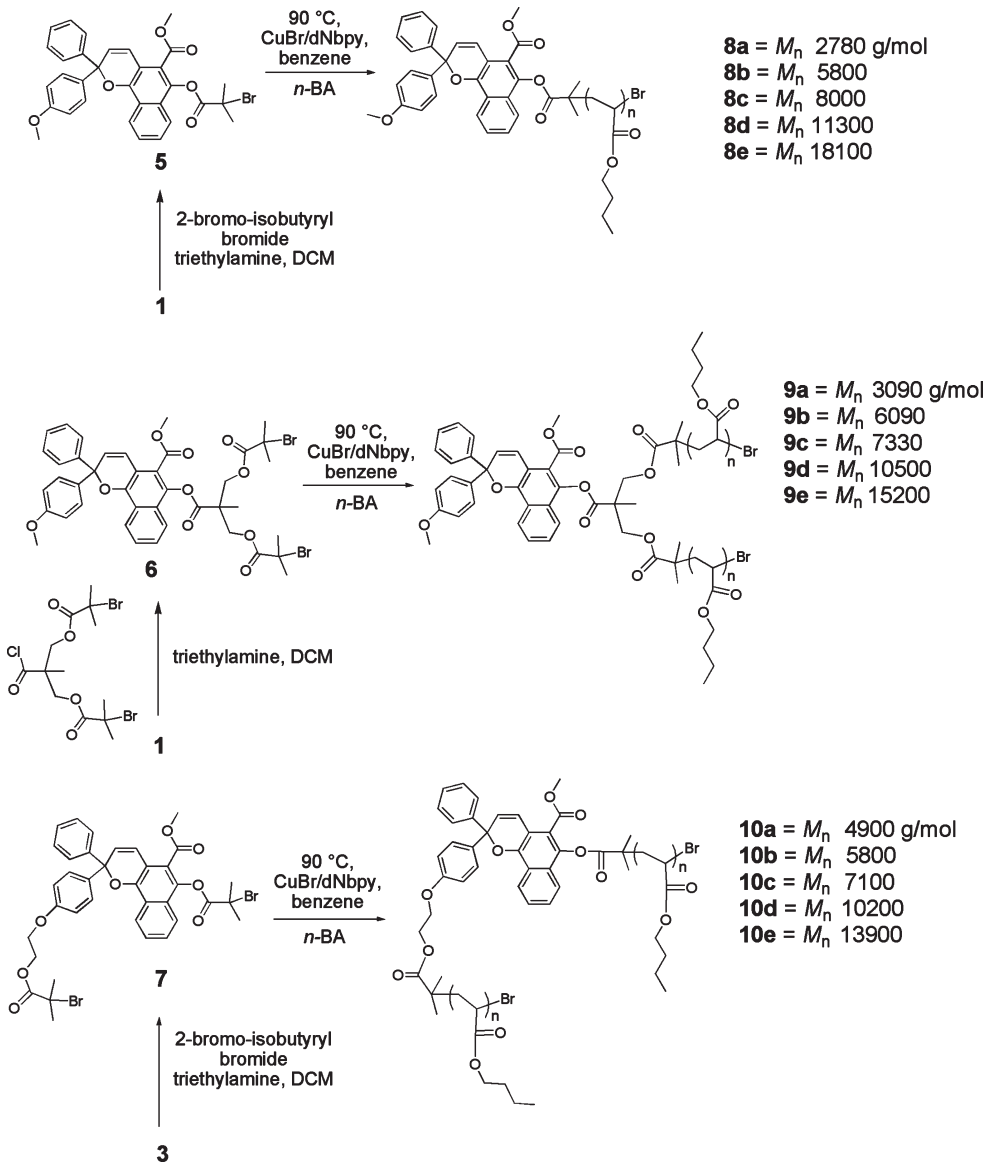


using 2-bromoisobutyryl bromide. The corresponding acid chloride was then coupled to the hydroxy-functionalized naphthopyran **1**.

**Naphthopyran−Polymer Conjugate Synthesis.** ATRP was used to synthesize various naphthopyran−p(*n*-BA) conjugates of increasing molecular weight ($M_n$, g/mol), as depicted in Scheme 2. All homopolymerizations were carried out in solution at 90 °C with CuBr and 4,4′-dinonyl-2,2′-bipyridine (dNbpy) as the catalyst system. In order to gauge the viability of these conditions, evolution plots were generated (Figures 3, 4, and 5). These displayed a linear progression of $M_n$ with conversion, with values similar to those expected theoretically for a controlled radical process and with low PDIs ($\leq$1.2) throughout. Furthermore, first-order kinetic plots for each of these polymerizations showed a near-linear relation with time (refer to Supporting Information). The specific characteristics of the polymerizations that generated the conjugates are shown in Table 1 and the final $M_n$ values of purified samples which were subsequently tested are displayed in Scheme 2. The corresponding GPC traces (shown in Supporting Information) display a high molecular weight shoulder for end-function polymers **8d** and **8e**. This can be attributed to long chain branching which occurs at higher conversions in polyacrylates as a result of backbiting and scission processes.[22]

Copolymerizations of naphthopyran acrylate **11** with *n*-BA were carried out using the same polymerization conditions (catalyst system, temperature, and solvent; see Figure 6) to yield **13a**−**13c**. Made only from acrylates, these copolymers are expected to contain a random distribution of naphthopyrans on each polymer chain. The final composition and molecular weights of each conjugate are shown in Scheme 3, their GPC traces and first-order kinetic plots are displayed in the Supporting Information, and their specific polymerization characteristics are shown in Table 1. Conversions were found to be no higher that 50%, even after 8 h, and in each case the remaining quantity of unreacted photochromic acrylate proved difficult to remove from the bulk polymer. In contrast, the purification of polymers made out of photochromic initiators was far less problematic since all photochromic moieties were utilized in the polymerization process.

A small proportion of naphthopyran methacrylate **12** was copolymerized with *n*-BA using difunctional ATRP

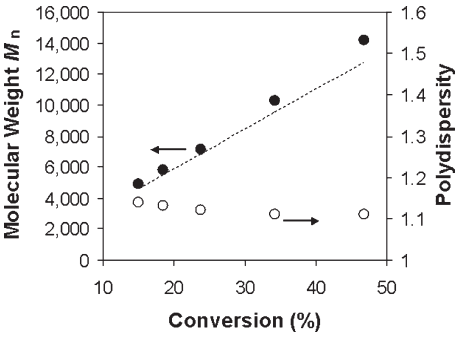


**Figure 4.** Evolution of polydispersity (○) and molecular weight (●) with conversion for the atom transfer radical polymerization of *n*-butyl acrylate with initiator **6** at 90 °C in benzene where [monomer]/[CuBr]/[4,4′-dinonyl-2,2′-bipyridine]/[6] = 200:1:2:1. Calculated molecular weight (---) by NMR conversion using the equation $M_n$ = ((monomer MW) × ([monomer]/[**6**]) × (NMR conversion)) + (MW of **6**). Polymerization times ranged from 1 to 3.5 h.

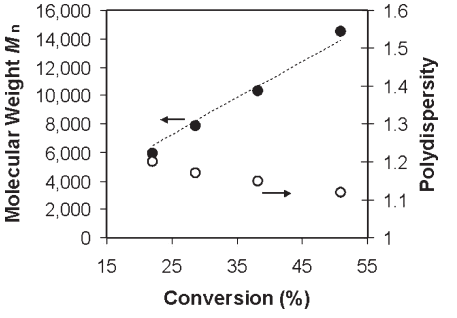


**Figure 5.** Evolution of polydispersity (○) and molecular weight (●) with conversion for the atom transfer radical polymerization of *n*-butyl acrylate with initiator **7** at 90 °C in benzene where [monomer]/[CuBr]/[4,4′-dinonyl-2,2′-bipyridine]/[**7**] = 200:1:2:1. Calculated molecular weight (---) by NMR conversion using the equation $M_n$ = ((monomer MW) × ([monomer]/[**7**]) × (NMR conversion)) + (MW of **7**). Polymerization times ranged from 1.3 to 5.7 h.

initiator, *n*-butyl 2,2-bis(2-bromo-2-methylpropanoyloxymethyl)propanoate (BBMPP) (Scheme 3), to yield **14a**. It was expected that an earlier and complete uptake of the naphthopyran monomer would occur since in this case its reactivity ratio in the copolymerization would be greater than that of *n*-BA.[23] Consequently, the crude polymerization mixture was found to contain no unreacted monomer by the end of the polymerization time (67% conversion). The difunctional nature of the ATRP initiator BBMPP also means that the naphthopyran moieties reside in the central portion of the polymer, within a Y-branched structure, depicted as "E" in Figure 2.

As shown in Scheme 4, several Y-branched midfunctional naphthopyran−p(*n*-BA)-conjugates were synthesized using difunctional initiator **6** and then chain extended with IBA to produce **15a**−**15c**. The initial homopolymerizations with *n*-BA were carried out in solution analogously to **9a**−**9e** and are labeled as p(*n*-BA) macroinitiator in Table 2. Block copolymer **16a** was made directly from conjugate **14a** as in Scheme 5. These ABA triblock copolymers, with naphthopyran/s contained within the middle soft section, were fabricated into films for testing.

The composition of the polymers was ascertained by $^1$H NMR, with specific examples displayed in the Supporting Information. Resonance peaks corresponding to the photochromic functionality as well as the initiator scaffold are evident in each. These aspects are confirmed by

**Table 1. Polymerization Characteristics of Naphthopyran−Poly(*n*-butyl acrylate) Conjugates**

| sample | type[a] | time (min)[b] | conv (%)[c] | [monomer]/[initiator] | exp $M_n$[d] | theor $M_n$[e] | PDI |
|---|---|---|---|---|---|---|---|
| **8a** | homopolym | 60 | 20 | 130 | 3360 | 3332 | 1.18 |
| **8b** | homopolym | 240 | 36 | 100 | 5710 | 5211 | 1.10 |
| **8c** | homopolym | 360 | 48 | 100 | 8150 | 6769 | 1.10 |
| **8d** | homopolym | 770 | 68 | 100 | 11600 | 9303 | 1.12 |
| **8e** | homopolym | 960 | 88 | 130 | 18700 | 15183 | 1.16 |
| **10a** | homopolym | 75 | 15 | 200 | 4900 | 4611 | 1.14 |
| **10b** | homopolym | 90 | 19 | 200 | 5800 | 5498 | 1.13 |
| **10c** | homopolym | 140 | 24 | 200 | 7100 | 6854 | 1.12 |
| **10d** | homopolym | 200 | 34 | 200 | 10200 | 9551 | 1.11 |
| **10e** | homopolym | 340 | 47 | 200 | 13900 | 12781 | 1.11 |
| **9a** | homopolym | 60 | 22 | 100 | 3820 | 3672 | 1.16 |
| **9b** | homopolym | 60 | 22 | 200 | 5940 | 6492 | 1.20 |
| **9c** | homopolym | 80 | 29 | 200 | 7830 | 8210 | 1.17 |
| **9d** | homopolym | 140 | 38 | 200 | 10300 | 10645 | 1.15 |
| **9e** | homopolym | 210 | 51 | 200 | 14500 | 13900 | 1.12 |
| **13a** | copolymer | 60 | 20 | 150 | 4270 | 4040 | 1.23 |
| **13b** | copolymer | 130 | 27 | 150 | 5950 | 5386 | 1.17 |
| **13c** | copolymer | 490 | 48 | 150 | 11500 | 9423 | 1.15 |
| **14a** | copolymer | 120 | 67 | 135 | 14400 | 12000 | 1.13 |

[a] Homopolym. = poly(*n*-butyl acrylate) homopolymer as shown in Scheme 2; copolymer = poly(*n*-butyl acrylate)-*co*-poly(naphthopyran) as shown in Scheme 3. [b] Polymerizations for **8a**−**8e** performed with *n*-butyl acrylate at 90 °C in benzene with [monomer]/[**5**] as indicated and [CuBr]/[4,4′-dinonyl-2,2′-bipyridine] = 1:2; polymerizations for **9a**−**9e** performed with *n*-butyl acrylate at 90 °C in benzene with [monomer]/[**6**] as indicated and [CuBr]/[4,4′-dinonyl-2,2′-bipyridine] = 1:2; polymerizations for **10a**−**10e** performed with *n*-butyl acrylate at 90 °C in benzene with [monomer]/[**7**] as indicated and [CuBr]/[4,4′-dinonyl-2,2′-bipyridine] = 1:2; polymerizations for **13a**−**13c** performed with *n*-butyl acrylate and **11** (98:2 by mole, respectively) at 90 °C in benzene with [monomers]/[ethyl 2-bromoisobutyrate] as indicated and [CuBr]/[4,4′-dinonyl-2,2′-bipyridine] = 1:2; polymerization for **14a** performed with *n*-butyl acrylate and **12** (99:1 by mole, respectively) at 90 °C in benzene with [monomers]/[BBMP] as indicated and [CuBr]/[4,4′-dinonyl-2,2′-bipyridine] = 1:2. [c] Determined by $^1$H NMR analysis of polymerization mixture. [d] Crude $M_n$ value, determined by GPC with THF as eluent with poly(*n*-butyl acrylate) equivalents obtained using Mark−Houwink parameters on a PS calibration. [e] Calculated based on monomer conversion plus initiator molecular weight (example $^1$H NMR spectra displayed in Supporting Information).

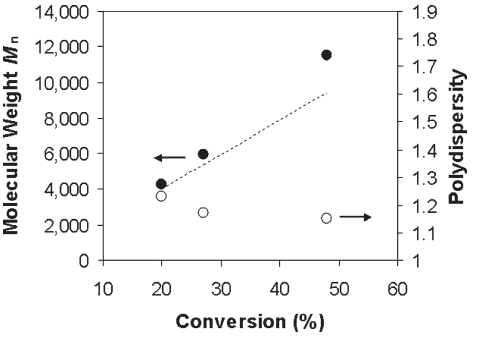


**Figure 6.** Evolution of polydispersity (○) and molecular weight (●) with conversion for the atom transfer radical copolymerization of *n*-butyl acrylate with monomer **11** (2%) at 90 °C in benzene, where [monomers]/[CuBr]/[4,4′-dinonyl-2,2′-bipyridine]/[ethyl 2-bromoisobutyrate initiator] = 150:1:2:1. Calculated molecular weight (---) by NMR conversion using the equation $M_n$ = {(*n*-butyl acrylate MW) × ([*n*-butyl acrylate]/[ethyl 2-bromoisobutyrate]) × (NMR conversion)} + {(**11** MW) × ([**11**]/[ethyl 2-bromoisobutyrate]) × (NMR conversion)} + (MW of ethyl 2-bromoisobutyrate). Polymerization times ranged from 1 to 8.2 h.

comparison of the spectrum of the conjugate with that of the initiator. The GPC traces showed successful block extension (Figures 7−10), a process that was made possible by

**Scheme 3. Atom Transfer Radical Polymerization Synthesis of Naphthopyran−Poly(*n*-butyl acrylate) Copolymers Displaying Molecular Weights and Compositions of Purified Samples Tested in Survey (NP = Naphthopyran Monomer, dNbpy = 4,4′-Dinonyl-2,2′-bipyridine)**

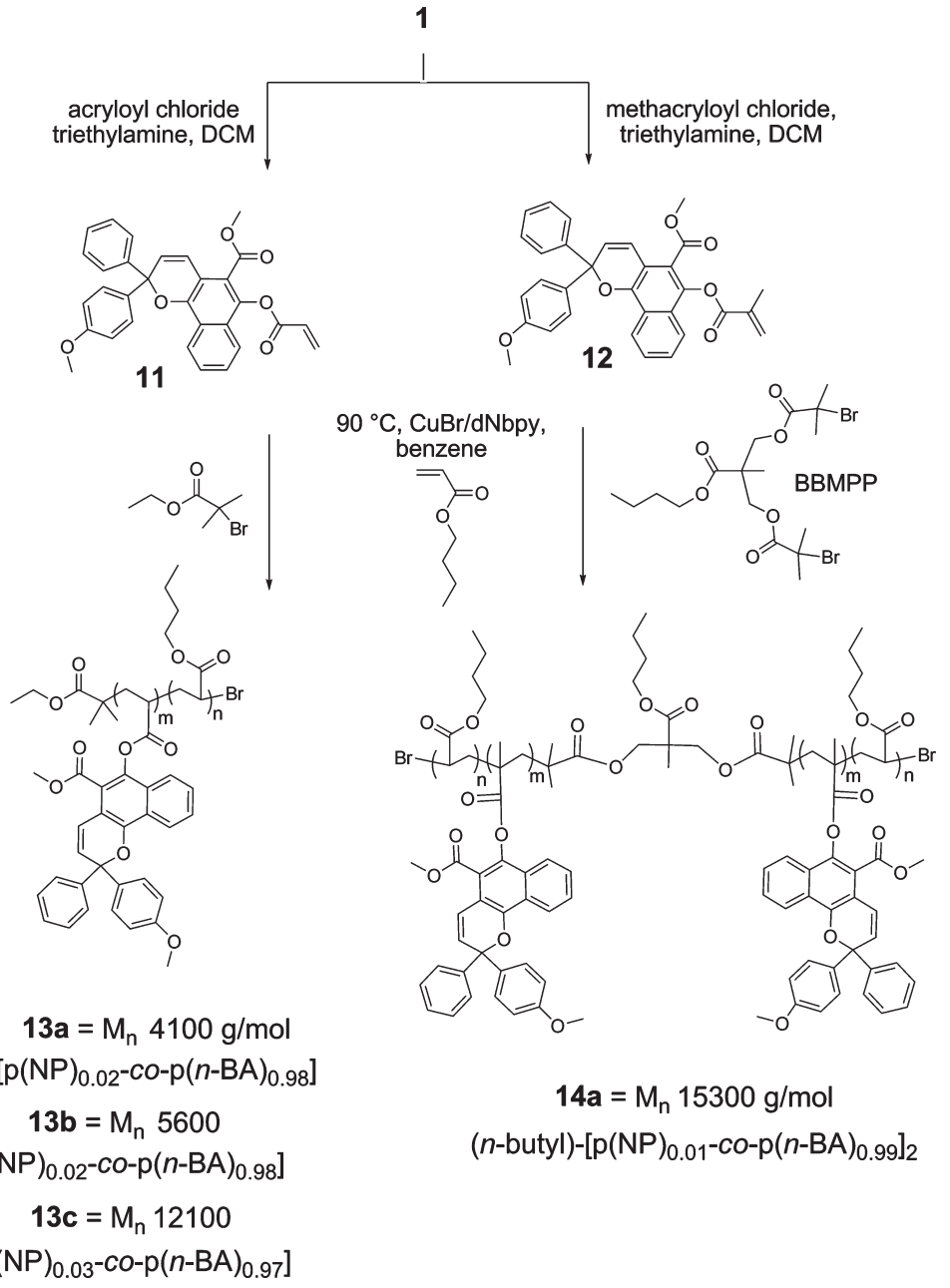


the living nature of ATRP. The polymers displayed good film processing properties and phase separated on annealing, as evidenced by DSC analysis which showed two separate glass transition temperatures ($T_g$) for each.

**Evaluation of Photochromic Performance.** *Cast-in Lenses.* The development of intense color in a photochromic test sample, either a cured lens or a cast film, is induced by incident irradiation with UV light. Upon cessation of the UV light the samples decolorize spontaneously in the dark due to the thermal back-reaction which occurs as the naphthopyran open form undergoes ring closure. Spectrokinetic properties can be studied by monitoring absorption density with time at the $\lambda_{max}$ of the colored form. The sample is continuously irradiated for 1000 s, and then the decoloration kinetics of the sample are investigated in the dark at 20 °C upon cessation of UV irradiation. The following empirical biexponential equation[4,24] was used to analyze the thermal ring closure kinetics of each sample:

$$A(t) = A_1 e^{-k_1 t} + A_2 e^{-k_2 t} + A_{th}$$

where $A(t)$ is the optical density at $\lambda_{max}$ of the open form; $A_1$ and $A_2$ are the contributions to the initial optical density $A_0$; $k_1$ and $k_2$ are exponential decay rate constants of fast and slow components respectively and $A_{th}$ is the residual coloration (offset).

The parameter $A_0$ which is also presented is the absorbance level achieved after 1000 s of continuous irradiation. This equation has been used frequently to represent and compare the decoloration behavior of both spirooxazines[11−13] and naphthopyrans[10,14,17] within solid media and has consistently fitted our decoloration curves with correlation coefficients ($R$) greater than 0.99.

Evaluation of $T_{1/2}$ values, which is the time taken for the sample to fade to half of initial absorbance value, provides insight into the overall kinetics. The photochromic properties of the lens samples are displayed in Table 3, and those of the cast films comprising the block copolymers are shown in Table 4.

Photochromic lens samples were prepared by adding the photochromic conjugates (or controls) individually to a lens monomer formulation at a set concentration level ($1.5 \times 10^{-7}$ mol of photochromic conjugate per gram of host matrix composition). This lens monomer formulation comprised poly(ethylene glycol) 400 dimethacrylate (PEGDMA) and 2,2′-bis(4-methacryloxyethoxy)phenylpropane (EBPDMA), 1:4 weight ratio, and with 0.4 mass % azobis(isobutyronitrile) (AIBN). The formulations were mixed thoroughly and thermally cured in a mold to produce optically clear test samples (as described in the Experimental Details).

Both end-functional and midfunctional naphthopyran–p(*n*-BA) conjugates displayed superior decoloration rates compared to their controls (Table 3). For each type the rates mildly increased with molecular weight of conjugated tail

**Scheme 4. Atom Transfer Radical Polymerization Synthesis of Naphthopyran ABA Triblock Copolymers 15a–15c (with Poly(isobornyl acrylate) as the A Block Sections and Poly(*n*-butyl acrylate) as the B Block Section), with Molecular Weights and Compositions of Purified Samples Tested[a]**

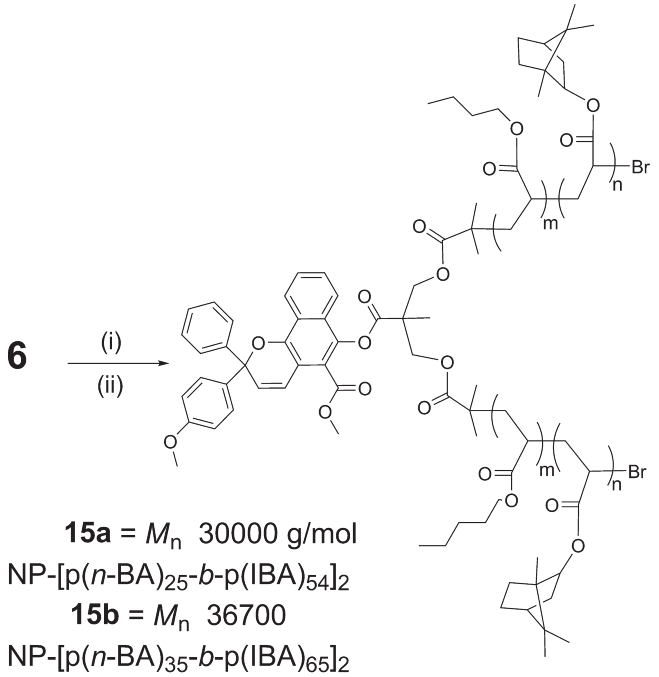


**15a** = $M_n$ 30000 g/mol
NP-[p(*n*-BA)$_{25}$-*b*-p(IBA)$_{54}$]$_2$
**15b** = $M_n$ 36700
NP-[p(*n*-BA)$_{35}$-*b*-p(IBA)$_{65}$]$_2$
**15c** = $M_n$ 28400
NP-[p(*n*-BA)$_{60}$-*b*-p(IBA)$_{30}$]$_2$

[a] (i) Polymerization of *n*-butyl acrylate with initiator **6** at 90 °C in benzene; (ii) block extension of purified poly(*n*-butyl acrylate) macroinitiator with isobornyl acrylate at 90 °C in benzene; refer to Table 2 for specific polymerization characteristics. NP = naphthopyran monomer, *n*-BA = *n*-butyl acrylate, IBA = isobornyl acrylate.

**Scheme 5. Atom Transfer Radical Polymerization Synthesis of Naphthopyran ABA Triblock Copolymer 16a (with Poly(isobornyl acrylate) as the A Block Sections and (Naphthopyran)-*co*-Poly(*n*-butyl acrylate) as the B Block Section), Displaying Molecular Weight and Composition of Purified Sample Tested (NP = Naphthopyran Monomer, *n*-BA = *n*-Butyl Acrylate, IBA = Isobornyl Acrylate)**

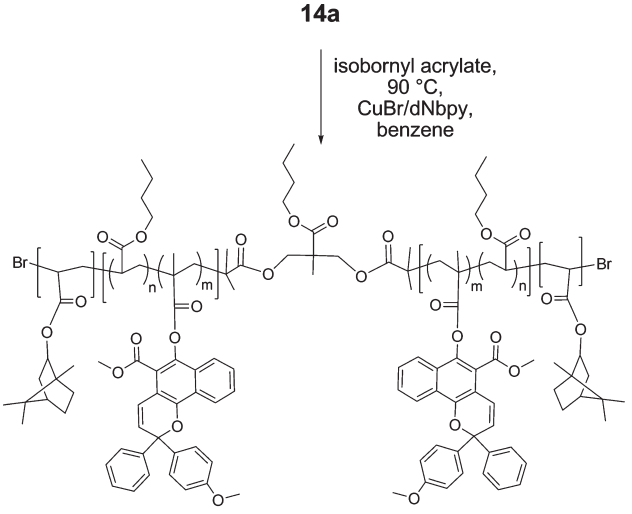


**16a** = $M_n$ 27000 g/mol
(*n*-butyl)-[(p(NP)$_{0.01}$-*co*-p(*n*-BA)$_{0.99}$)-*b*-p(IBA)]$_2$
*n*-BA units = 58 x 2
IBA units = 28 x 2

**Table 2. Polymerization Characteristics of Naphthopyran–Poly(*n*-butyl acrylate)-*b*-Poly(isobornyl acrylate) Triblock Copolymers**

| type | time (min)[a] | conv (%)[b] | [monomer]/[initiator] | exp $M_n$[c] | theor $M_n$[d] | PDI | $T_g$ (°C)[e] |
|---|---|---|---|---|---|---|---|
| p(*n*-BA) macroinitiator | 60 | 52 | 100 | 7270 | 7530 | 1.13 | |
| **15a** | 250 | 61 | 154 | 30000 | 26800 | 1.24 | −46, 47 |
| p(*n*-BA) macroinitiator | 80 | 35 | 200 | 9740 | 9825 | 1.19 | |
| **15b** | 250 | 67 | 150 | 36700 | 30500 | 1.22 | −48, 48 |
| p(*n*-BA) macroinitiator | 170 | 58 | 200 | 16500 | 15759 | 1.14 | |
| **15c** | 250 | 42 | 144 | 28400 | 28800 | 1.17 | −41, 74 |
| **16a** | 220 | 40 | 150 | 27000 | 28000 | 1.17 | −44, 80 |

[a] For **15a** polymerization of *n*-butyl acrylate with initiator **6** at 90 °C in benzene, where [monomer]/[CuBr]/[4,4′-dinonyl-2,2′-bipyridine]/[**6**] = 100:1:2:1, and block extension of purified poly(*n*-butyl acrylate) macroinitiator with isobornyl acrylate at 90 °C in benzene, where [monomer]/[CuBr]/[4,4′-dinonyl-2,2′-bipyridine]/[macroinitiator] = 154:1:2:1; For **15b** polymerization of *n*-butyl acrylate with initiator **6** at 90 °C in benzene where [monomer]/[CuBr]/[4,4′-dinonyl-2,2′-bipyridine]/[**6**] = 200:1:2:1, and block extension of purified poly(*n*-butyl acrylate) macroinitiator with isobornyl acrylate at 90 °C in benzene, where [monomer]/[CuBr]/[4,4′-dinonyl-2,2′-bipyridine]/[macroinitiator] = 150:1:2:1; For **15c** polymerization of *n*-butyl acrylate with initiator **6** at 90 °C in benzene, where [monomer]/[CuBr]/[4,4′-dinonyl-2,2′-bipyridine]/[**6**] = 200:1:2:1, and block extension of purified poly(*n*-butyl acrylate) macroinitiator with isobornyl acrylate at 90 °C in benzene, where [monomer]/[CuBr]/[4,4′-dinonyl-2,2′-bipyridine]/[macroinitiator] = 144:1:2:1; For **16a** block extension of p(*n*-butyl acrylate) macroinitiator **14a** (see polymerization characteristics shown in Table 1) with isobornyl acrylate at 90 °C in benzene where [monomer]/[CuBr]/[4,4′-dinonyl-2,2′-bipyridine]/[macroinitiator] = 150:1:2:1. [b] Determined by $^1$H NMR analysis of polymerization mixture. [c] For *p*(*n*-butyl acrylate) macroinitiator determined by GPC with THF as eluent with poly(*n*-butyl acrylate) equivalents obtained using Mark–Houwink parameters on a PS calibration; for block copolymers estimated by $^1$H NMR of purified samples. [d] Calculated based on monomer conversion plus macroinitiator molecular weight. Example $^1$H NMRs displayed in the Supporting Information. [e] Two $T_g$ values determined by DSC; refer to Experimental Details.

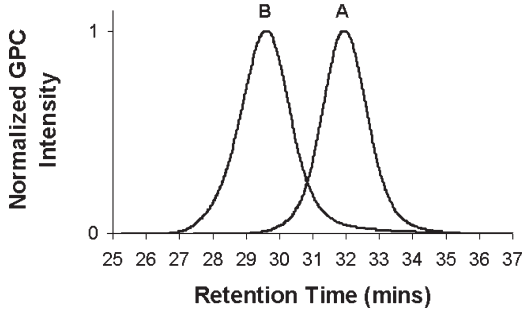


**Figure 7.** Overlaid and normalized GPC traces of each step of block copolymer formation. Peak A = midfunctional naphthopyran−poly(*n*-butyl acrylate) macroinitiator; peak B = naphthopyran−poly(*n*-butyl acrylate)-*b*-poly(isobornyl acrylate) triblock copolymer, **15a** (shown in Scheme 4).

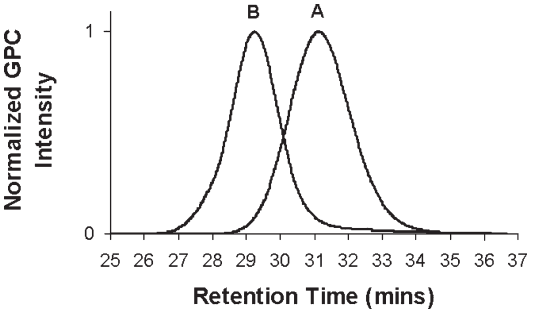


**Figure 8.** Overlaid and normalized GPC traces of each step of block copolymer formation. Peak A = midfunctional naphthopyran−poly(*n*-butyl acrylate) macroinitiator; peak B = naphthopyran−poly(*n*-butyl acrylate)-*b*-poly(isobornyl acrylate) triblock copolymer, **15b** (shown in Scheme 4).

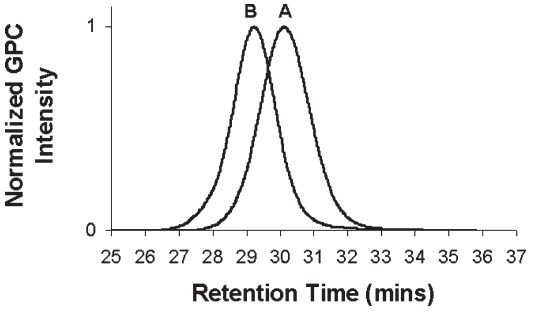


**Figure 9.** Overlaid and normalized GPC traces of each step of block copolymer formation. Peak A = midfunctional naphthopyran−poly(*n*-butyl acrylate) macroinitiator; peak B = naphthopyran−poly(*n*-butyl acrylate)-*b*-poly(isobornyl acrylate) triblock copolymer, **15c** (shown in Scheme 4).

showing that chain length can be used to finely tune the rate of decay. We have found that when a short and hard block segment is inserted near a photochromic, followed by a lubricating section, this allows a much wider range of switching speeds to be accessed.[25] This has also been the case when an aromatic Y-branching linker is used to synthesize midfunctional p(*n*-BA) conjugates.[14] In light of these results, the level of tunability appears to be dependent on the nature of the linker near the photochromic moiety.

As seen in Figure 11, a comparison of the decoloration performance of end-functionalized conjugates **8a**−**8e** with that of mid-functionalized conjugates, **9a**−**9e** and **10a**−**10e**, shows that when the photochromic is positioned in the center of the chain, it responds favorably with lower $T_{1/2}$ values and with an overall improved performance per chain length.

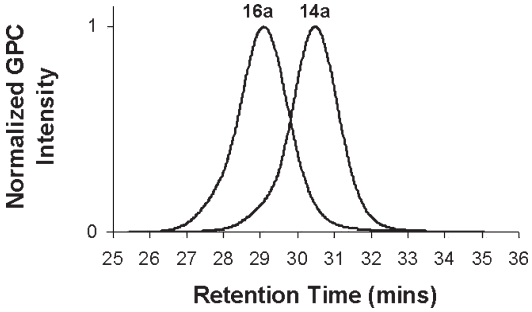


**Figure 10.** Overlaid and normalized GPC traces of each step of block copolymer formation for **16a** (as shown in Scheme 5).

Therefore, two polymer chains per photochromic moiety provides better encapsulation within the rigid host matrix. Furthermore, placing the photochromic pendant from the chain, as **9a**−**9e**, gives superior performance compared to directly placing it within the chain, as **10a**−**10e**.

This is also reflected in the major rate constant $k_1$, which, when compared directly to that of the control, is markedly higher for midfunctional conjugates **9a**−**9e** (Figure 12). The values in fact start to approach twice the value of the control ($k_1 = 0.595\ \text{min}^{-1}$) and this effect arises at a relatively modest molecular weight of conjugated tail (e.g., **9d** with $M_n$ 10 500 g/mol, $k_1 = 1.116\ \text{min}^{-1}$). Coloration values, $A_0$, of samples prepared from conjugates **8a**−**8e**, **9a**−**9e**, and **10a**−**10e**, which have exactly one dye moiety per polymer chain, can be directly compared to that of their controls since they all contained equivalent concentrations of dye. As seen in Table 3, the values for these conjugates were 1.1−1.3 times greater than their controls. This is in agreement with previous work which showed that a higher level of coloration was associated with samples that displayed faster kinetics.[14]

Naphthopyran−p(*n*-BA) linear random copolymers **13a**−**13c** showed decay speeds comparable to the midfunctional (homopolymer) conjugates, **10a**−**10e**; however, per chain length their performance was found to be superior to that of end-functional conjugates, **8a**−**8e**. This is also in agreement with previous results which compared various naphthopyran copolymers with end-functional conjugates[10] and can be ascribed to greater association of pendant naphthopyran moieties with neighboring *n*-BA units within the copolymer. Interestingly, increases in chain length were correlated with a tuning down of response ($k_1$ goes down from **13a** to **13c**). This is most likely due to increasing naphthopyran units per chain along the series that would decrease chain mobility. Therefore, from the point of view of incomplete uptake of monomer units during the copolymerization and an inability to regulate the exact location of the dye in the chain, this approach is less attractive overall compared to Y-branching architecture (**9a**−**9e**) which provides both a precise and well-encapsulated location for the dye in the chain.

Copolymer **14a** also incorporates a Y-branched structure where the naphthopyran moieties reside in the central portion of the polymer, as depicted in Figure 2 and Scheme 3. Its kinetics within the host matrix were in fact superior to those of all the linear copolymers, **13a**−**13c**, indicating that this system offers better encapsulation per chain length.

Hypsochromic (blue) shifts in wavelength of the colored form were seen for the photochromic conjugates in the host matrix compared to the controls. This can be attributed to effective shielding of naphthopyran moieties, as a result of conjugation to p(*n*-BA), from the more polar matrix environment that comprises substantial PEG units. This is

**Table 3. Photokinetic Analysis of the Decoloration of Poly(*n*-Butyl acrylate)−Naphthopyran Conjugates and Their Corresponding Controls in Host Matrix (PEGMA:EBPDMA 1:4 Mass Composition)[a]**

| sample | $\lambda_{max}$ (nm) | $M_n$[b] | $A_0$[c] | $k_1$ ($min^{-1}$) | $A_1$ | $k_2$ ($min^{-1}$) | $A_2$ | $A_{th}$ | $t_{1/2}$ (s)[d] |
|---|---|---|---|---|---|---|---|---|---|
| **2** | 500 | | 0.93 | 0.6095 | 0.6415 | 0.0699 | 0.0975 | 0.2394 | 123.0 |
| **8a** | 500 | 2780 | 1.02 | 0.7356 | 0.7117 | 0.0743 | 0.0478 | 0.2226 | 88.5 |
| **8b** | 496 | 5800 | 1.06 | 0.7920 | 0.7321 | 0.0864 | 0.0331 | 0.2216 | 79.5 |
| **8c** | 496 | 8000 | 1.11 | 0.8192 | 0.7368 | 0.0844 | 0.0303 | 0.2229 | 76.5 |
| **8d** | 495 | 11300 | 1.11 | 0.8801 | 0.7124 | 0.7138 | 0.0555 | 0.2260 | 75.0 |
| **8e** | 495 | 18100 | 1.19 | 0.8543 | 0.7396 | 0.0556 | 0.0253 | 0.2225 | 73.2 |
| **4** | 500 | | 0.90 | 0.5943 | 0.6334 | 0.0763 | 0.1127 | 0.2346 | 130.0 |
| **10a** | 492 | 4900 | 1.06 | 0.8151 | 0.7461 | 0.0878 | 0.0318 | 0.2096 | 75.0 |
| **10b** | 492 | 5800 | 1.09 | 0.8483 | 0.7594 | 0.0634 | 0.0213 | 0.2080 | 70.5 |
| **10c** | 492 | 7100 | 1.07 | 0.8800 | 0.7608 | 0.0551 | 0.0202 | 0.2063 | 67.5 |
| **10d** | 492 | 10200 | 1.04 | 0.8782 | 0.7677 | 0.0534 | 0.0194 | 0.2005 | 66.0 |
| **10e** | 492 | 13900 | 1.09 | 0.8961 | 0.7658 | 0.0723 | 0.0206 | 0.2037 | 66.0 |
| **2** | 500 | | 0.92 | 0.5950 | 0.6630 | 0.0856 | 0.1004 | 0.2184 | 120.0 |
| **9a** | 497 | 3090 | 1.11 | 1.0319 | 0.7352 | 0.0740 | 0.0237 | 0.2297 | 62.0 |
| **9b** | 495 | 6090 | 1.08 | 1.0267 | 0.7374 | 0.0774 | 0.0238 | 0.2307 | 62.0 |
| **9c** | 495 | 7330 | 1.21 | 1.0647 | 0.7356 | 0.0648 | 0.0231 | 0.2304 | 59.0 |
| **9d** | 495 | 10500 | 1.19 | 1.1159 | 0.7439 | 0.0505 | 0.0185 | 0.2268 | 56.0 |
| **9e** | 495 | 15200 | 1.21 | 1.1168 | 0.7453 | 0.0658 | 0.0171 | 0.2285 | 56.0 |
| **13a** | 495 | 4100 | 0.80 | 0.9216 | 0.7435 | 0.0414 | 0.0248 | 0.2174 | 66.0 |
| **13b** | 495 | 5600 | 1.01 | 0.8642 | 0.7351 | 0.0736 | 0.0361 | 0.2189 | 73.2 |
| **13c** | 495 | 12100 | 1.76 | 0.8406 | 0.7544 | 0.0887 | 0.0333 | 0.1999 | 70.5 |
| **14a** | 495 | 15300 | 1.92 | 0.9802 | 0.7316 | 0.1727 | 0.0513 | 0.2120 | 65.0 |

[a] Samples initially irradiated at 350−400 nm for 1000 s, then decoloration monitored at $\lambda_{max}$ of the colored form (predetermined by wavelength scan of colored form) at 20 °C in the dark for 4800 s. [b] Molecular weight ($M_n$, g/mol) of purified conjugates estimated from GPC analysis: poly(*n*-butyl acrylate) equivalents obtained using Mark−Houwink parameters on a PS calibration. [c] Measured absorbance intensity at onset of thermal decoloration period. [d] Time taken for the initial absorbance value, $A_0$, to decay to half its original value.

**Table 4. Photokinetic Analysis of the Decoloration of Naphthopyran Tribock Copolymer Films**

| sample | $\lambda_{max}$ (nm) | $M_n$[b] | [*n*-BA]/[IBA] | $A_0$[c] | $k_1$ ($min^{-1}$) | $A_1$ | $k_2$ ($min^{-1}$) | $A_2$ | $A_{th}$ | $t_{1/2}$ (s)[d] |
|---|---|---|---|---|---|---|---|---|---|---|
| **15a** | 488 | 30000 | 1: 2 | 1.19 | 0.5215 | 0.5418 | 0.0646 | 0.1996 | 0.2180 | 178.0 |
| **15b** | 488 | 36700 | 1: 1.9 | 2.00 | 0.6680 | 0.6410 | 0.0739 | 0.1345 | 0.1954 | 110.0 |
| **15c** | 488 | 28400 | 2: 1 | 1.42 | 0.9743 | 0.7860 | 0.0249 | 0.0149 | 0.1968 | 60.0 |
| **16a** | 488 | 27000 | 2.1: 1 | 1.27 | 0.7360 | 0.7542 | 0.0804 | 0.0515 | 0.1756 | 80.0 |

[a] Samples initially irradiated at 350−400 nm for 1000 s, then decoloration monitored at $\lambda_{max}$ of the colored form (predetermined by wavelength scan of colored form) at 20 °C in the dark for 4800 s. [b] Molecular weight ($M_n$, g/mol) of purified block copolymers estimated from $^1$H NMR. [c] Measured absorbance intensity at onset of thermal decoloration period. [d] Time taken for the initial absorbance value, $A_0$, to decay to half its original value.

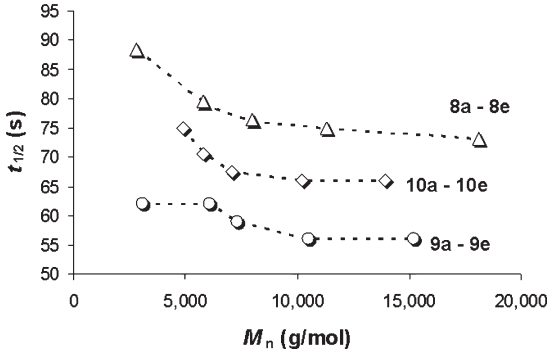


**Figure 11.** Thermal decoloration comparison: measured $T_{1/2}$ values (in seconds) of naphthopyran−poly(*n*-butyl acrylate) conjugates (**8a−8e, 9a−9e**, and **10a−10e**) vs their corresponding molecular weight when cast in the host matrix, PEGDMA:EBPDMA (1:4).

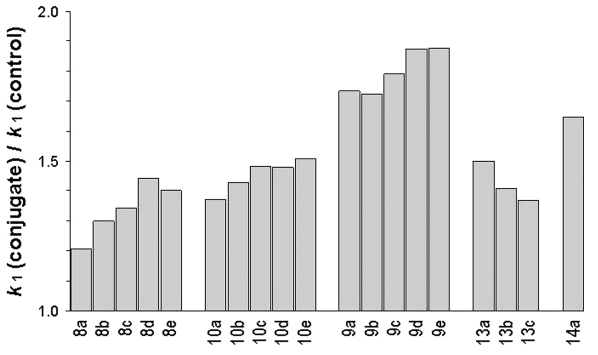


**Figure 12.** Thermal decoloration comparison: $k_1$(conjugate)/$k_1$-(control) of naphthopyran−poly(*n*-butyl acrylate) conjugates (**8a−8e, 9a−9e, 10a−10e, 13a−13c**, and **14a**) when cast in the host matrix PEGDMA:EBPDMA (1:4).

particularly evident for conjugates **10a−10e** which displayed the largest shift (492 nm) indicating a significant insulation and encapsulation effect. However, given that these structures were second best overall in terms of enhancing kinetics, the weight of two polymer chains radiating from a central, nonpendant photochromic moiety seems to offset this benefit. Overall, Y-branched structures **9a−9e**, which contain two polymer arms per midfunctional and pendant photochromic moiety, displayed the fastest kinetics and the most impressive colorabilities.

In previous studies the $T_{1/2}$ value for the naphthopyran control dye **2** measured in toluene at 20 °C was found to be 63 and 52 s for its corresponding propionate derivative.[10,17] The ability of the photochromic−polymer conjugates in a rigid host to surpass solution kinetics is unlikely, strongly suggesting that the Y-branching technology presented here, which achieved a $T_{1/2}$ value of 56 s (for **9d** and **9e**), has reached a limit. Extra branching points are unlikely to offer additional kinetic benefits.

In conclusion, these results show that by changing the arrangement and geometry of units comprising the photochromic−polymer conjugate, one can further tune the switching behavior within a rigid host, and this is possible without making modifications to the bulk host material.

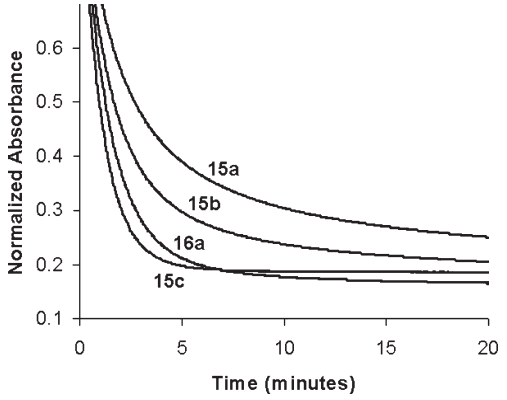


**Figure 13.** Thermal decoloration curves (monitored in the dark at 20 °C after UV irradiation for 1000 s) of naphthopyran−p(*n*-butyl acrylate)-*b*-p(isobornyl acrylate) block copolymers. Refer to Schemes 4 and 5 and Table 4 for sample description.

*Photochromic Films: ABA Triblock Copolymers*. The tuning of naphthopyran switching in bulk films has already been achieved using block copolymers synthesized using reversible addition−fragmentation chain transfer (RAFT) polymerization.[26] These structures were linear block copolymers made with naphthopyran monomers copolymerized into the soft poly(methyl acrylate) sections of the block copolymers. The hard sections comprised either polystyrene or poly(methyl methacrylate), both optically clear, high-$T_g$ polymers. Controlled radical polymerization techniques can be used to synthesize hard−soft block copolymers that phase separate with the photochromic encapsulated into the low-$T_g$ environment of the soft phase. The soft local environment allows switching speed to be enhanced while the continuous high-$T_g$ matrix maintains structural integrity at higher than ambient temperatures. This approach was explored in this paper using ATRP with the formation of ABA triblock copolymers with a promising arrangement and choice of building units for photochromic kinetics where Y-branched naphthopyran−p(*n*-BA) macroinitiators were block extended with p(IBA) (Schemes 4 and 5). An ideal system of encapsulation for the dye was afforded by its midplacement within the fluid phase of p(*n*-BA), and the surrounding p(IBA) was chosen as the hard section of the block copolymers because of its high $T_g$, hardness, comparable properties to poly(methyl methacrylate) and polystyrene, and ease of polymerization.[27] Films of the block copolymers were prepared by casting followed by annealing for 16 h. The photochromic properties of films comprised of **15a**−**15c** and block copolymer **16a**, the latter made from Y-branched p(*n*-BA) macroinitiator **14a**, are presented in Table 4.

The overlaid thermal decolorization curves of the block copolymer films, shown as Figure 13, clearly show that a high level of tuning is achievable using this approach, and it is the composition of the block copolymers that is primarily implicated; the fastest decolorization time was achieved for **15c** ($T_{1/2}$ 60 s), which contained the highest proportion of p(*n*-BA) and the highest quantity of *n*-BA repeat units and the slowest time was achieved by the **15a** ($T_{1/2}$ 178 s) which contained the lowest proportion of p(*n*-BA) and also the lowest quantity of *n*-BA repeat units. As distinct from the casting-in method described above, here the photochromic conjugates themselves comprise the matrix. The extent of separation of the photochromic moieties from the hard p(IBA) component is therefore highly dependent on the amount of p(*n*-BA) encapsulating them.

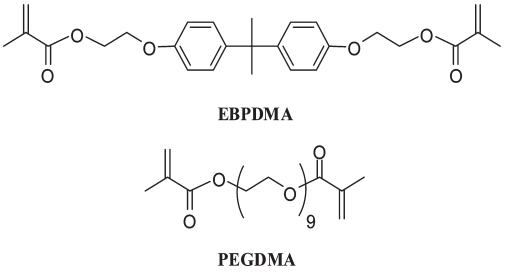


**Figure 14.** Structures of monomers of thermally curable host matrix formulation.

The film comprised of **16a**, which also contained a high proportion of p(*n*-BA), was second in speed to **15c** ($T_{1/2}$ 80 s vs $T_{1/2}$ 60 s). Furthermore, **14a**, which is the precursor to **16a**, displayed a higher coloration value, $A_0$, in the lens compared to all the conjugates, indicating more than one naphthopyran moiety is present per chain. As described above, the photochromic moieties of this conjugate reside within the central part of the polymer with proximity to one another, which increases their local rigidity and reduces the mobility of polymer chains. With reference to Table 3, this is supported by the fact that the decolorization behavior of **14a** within the lens matrix is a lot slower than conjugate **9e** ($T_{1/2}$ 65 s vs $T_{1/2}$ 56 s), even though both have approximately the same molecular weight.

Lastly, these studies display an overall tendency of the casting-in method to provide faster kinetics in comparison to the films. The macroinitiators used to synthesize block copolymers **15a**−**15c** had the same structures and similar $M_n$ values (7270−16 200 g/mol) as **9c**−**9e** ($M_n$ 7330−15 200 g/mol). However, the corresponding block copolymer films of **15a**−**15c** displayed slower kinetics ($k_1 = 0.52-0.97$ min$^{-1}$) compared with the lens kinetics displayed by conjugates **9c**−**9e** ($k_1 = 1.06-1.12$ min$^{-1}$). Furthermore, comparing the kinetics of **14a** in the lens matrix ($k_1 = 0.98$ min$^{-1}$) with that of the film **16a** ($k_1 = 0.74$ min$^{-1}$), the same trend is displayed. The lens host is a continuous cross-linked network with a measured $T_g$ of ~120 °C,[9] so chain mobility within the local environment of the photochromic rests heavily on the ability of p(*n*-BA) to partition away from the host matrix. This will be enhanced by the discontinuity and incompatibility between the two components. However, in the case of the films, the block copolymer comprises the bulk matrix, where the ability of the two phases to effectively separate is critical and therefore highly dependent on processing conditions. In order to bring kinetics between the two matrices closer together, this aspect could be further examined.

## Conclusion

ATRP was used to synthesize naphthopyran−polymer conjugates of a variety of architectures. First, within a lens rigid matrix, an investigation of various p(*n*-BA) homopolymers showed that a midfunctional placement of the dye, made possible with a difunctional photochromic initiator, gave superior kinetics per chain length of conjugated polymer. Moreover, it was preferable to have the dye pendant from the chain as opposed to directly within the chain. Analysis of naphthopyran−p(*n*-BA) copolymers showed that having the dye pendant from the chain as a monomer was also attractive; however, the ability to tune response via chain length was not possible using random copolymers made with a naphthopyran acrylate. A better approach was to use a gradient copolymer system with a nonphotochromic difunctional initiator that allowed total incorporation of the

naphthopyran methacrylate within the middle portion of the polymer.

The formation of copolymers with the photochromic encapsulated in the middle of a Y-branched central soft section was made possible using an ABA triblock geometry. Their described films showed enhanced tuning of response dependent on the overall proportion of soft section inhabited by the photochromic.

It is interesting that regardless of the method used to assemble a photochromic material, such as casting in a lens or film formation, the ability to manipulate polymer architecture is appealing because it provides an extra avenue to control photochromic properties, beyond chain length and rigidity ($T_g$).

## Experimental Details

**Materials.** The synthesis of methyl 6-hydroxy-2-(4-methoxyphenyl)-2-phenyl-2*H*-naphtho[1,2-*b*]pyran-5-carboxylate (**1**), methyl 6-(isobutyryloxy)-2-(4-methoxyphenyl)-2-phenyl-2*H*-naphtho[1,2-*b*]pyran-5-carboxylate (**2**), methyl 6-(2-bromo-2-methylpropanoyloxy)-2-(4-methoxyphenyl)-2-phenyl-2*H*-naphtho[1,2-*b*]pyran-5-carboxylate (**5**), methyl 6-(acryloyl)-2-(4-methoxyphenyl)-2-phenyl-2*H*-naphtho[1,2-*b*]pyran-5-carboxylate (**11**), and methyl 6-(methacryloyl)-2-(4-methoxyphenyl)-2-phenyl-2*H*-naphtho[1,2-*b*]pyran-5-carboxylate (**12**) has been described by us previously in the literature.[10] 2,2-Bis(2-bromo-2-methylpropanoyloxymethyl)propanoic acid was prepared using a procedure adapted from the literature.[19−21] All chemicals (reagents and solvents) used for synthesis were of high purity and used as received unless otherwise stated. *n*-Butyl acrylate (99+% purity, Aldrich) was purified by passing through aluminum oxide 90, activated basic (0.063−0.200 nm, Merck) to remove inhibitors and then flash vacuum distilled prior to use. Isobornyl acrylate (tech grade, Aldrich) was purified by passing through aluminum oxide 90, activated basic (0.063−0.200 nm, Merck) to remove inhibitors. All reagents were purchased from Aldrich Chemical Co. unless otherwise stated. All chromatography was performed using silica gel (Kieselgel Merck 60, 0.040−0.063 mm), and TLC was performed on Merck Silica $60F_{254}$ plates.

**General Experimental Measurements.** Gel permeation chromatography (GPC) was performed on a Waters 515 HPLC pump and Waters 717 Plus Autosampler equipped with Waters 2414 refractive index detector and 3 × Mixed-C (7.5 mm × 300 mm, 5 $\mu$m particle size, linear molecular weight range 200−2 000 000) and 1 Mixed E PLgel column (7.5 mm × 300 mm, 3 $\mu$m particle size, linear molecular weight range up to 30 000) from Polymer Laboratories. Tetrahydrofuran (THF) with a flow rate of 1.0 mL $min^{-1}$ was used as eluent at 22 ± 2 °C. Molecular weights for p(*n*-BA)−naphthopyran conjugates were calculated via calibration with narrow polydispersity polystyrene standards (Polymer Laboratories) ranging from 600 to 7.5 × $10^6$ g/mol. Molecular weights ($M_n$) were converted to p(*n*-BA) equivalents using Mark−Houwink parameters[28] on the PS calibration. Number ($M_n$)- and weight-average ($M_w$) molecular weights were evaluated using Waters Millennium/Empower software. A third-order polynomial was used to fit the log *M* vs time calibration curve, which was linear across the molecular weight ranges.

$^1$H (400 MHz) and $^{13}$C NMR (100 MHz) spectra were obtained with a Bruker Av400 spectrometer at 25 °C. Spectra were recorded for samples dissolved in deuterated solvent, and chemical shifts are reported as parts per million from external tetramethylsilane. Monomer conversions were obtained from the $^1$H NMR spectra. The resonances integrated to obtain conversions for *n*-BA polymerizations were the vinyl peaks at 5.8, 6.2, and 6.4 ppm (monomer only) and the $OCH_2-$ peaks at 3.9−4.1 ppm (monomer and polymer). The resonances integrated to obtain conversions for IBA polymerizations were the vinyl peaks at 5.8, 6.2, and 6.4 ppm (monomer only) and the isobornyl −CH− peak at 4.60−4.85 ppm (monomer and polymer). The compositional ratio of the copolymers (including triblocks) was calculated by $^1$H NMR via the integrated peak intensity ratio of naphthopyran vs that of the polymers. All other spectra were recorded on a Bruker Av400 spectrometer.

Positive ion EI mass spectra were run on a ThermoQuest MAT95XL mass spectrometer using ionization energy of 70 eV. Accurate mass measurements were obtained with a resolution of 5000−10000 using PFK as the reference compound.

Thermal analysis by differential scanning calorimetry (DSC) was performed in order to determine the $T_g$ of the triblock copolymers. This was carried out using a Mettler Toledo DSC821 machine with temperature and heat flow calibrated using indium and zinc as reference substances. Samples (~10 mg) were heated under nitrogen from −50 to 150 °C at 10 °C/min. The $T_g$ values were taken from the midpoints of the heat flow changes observed in the second heat cycle.

**Photochromic Analysis.** Under continuous UV irradiation, the photochromic responses of the samples (cured lenses or cast films) were analyzed on a light table composed of a Cary 50 spectrophotometer to measure the absorbance and a 160 W Oriel xenon lamp as an incident light source. A series of two filters (Edmund Optics 320 cutoff and bandpass filter U-340) were used to restrict the output of the lamp to a narrow band (350−400 nm). The samples were maintained at 20 °C and monitored at their maximum absorbance of the colored form for a period of 1000 s. Then the thermal decoloration was monitored in the absence of UV irradiation for a further 6000 s.

**Synthesis of 6-Hydroxy-2-(4-(2-hydroxyethoxy)phenyl)-2-phenyl-2*H*-naphtho[1,2-*b*]pyran-5-carboxylate (3).** The complete procedure for synthesis of the title compound can be derived from what is already reported in the literature.[17] 4-Hydroxybenzophenone was first converted to 4-(2-hydroxyethoxy)benzophenone using bromoethanol and $Na_2CO_3$. This was then converted to 1-(2-hydroxyethoxy)phenyl)-1-phenyl-prop-2-yn-1-ol using 2 mol equiv of (trimethylsilyl)acetylene and *n*-butyllithium (1.6 M in hexane) with respect to the benzophenone. The title compound was then derived from 1-(2-hydroxyethoxy)phenyl)-1-phenyl-prop-2-yn-1-ol and methyl 1,4-dihydroxynapthalene-2-carboxylate, after purification by column chromatography (silica gel 60, ethyl acetate/hexane) as a bright yellow solid (2.3 g, 75%). $^1$H NMR (400 MHz, $d_6$-acetone) $\delta$: 3.80−3.83 (m, 2H, $CH_2CH_2OH$), 3.87 (t, 1H, *J* 5.80 Hz, OH), 4.00 (t, 2H, *J* 4.85 Hz, $CH_2CH_2OH$), 4.06 (s, pyran-CH, $COOCH_3$), 6.38 (d, *J* 10.0 Hz, 1H, pyran-CH), 6.87 (apparent d, *J* 8.8 Hz, 2H, ArH), 7.22−7.26 (m, 1H, ArH), 7.31−7.35 (m, 2H, ArH), 7.47 (apparent doublet, *J* 8.8 Hz, 2H, ArH), 7.52 (d, *J* 10.0 Hz, 1H, pyran-CH), 7.56−7.63 (m, 3H, ArH), 7.75−7.79 (m, 1H, ArH) 8.32 (d, *J* 8.4 Hz, 1H, ArH), 8.42 (d, *J* 8.4 Hz, 1H, ArH), 12.17 (s, 1H, ArOH). $^{13}$C NMR (100 MHz, $d_6$-acetone) $\delta$: 53.8, 62.1, 71.3, 82.7, 104.0, 115.3, 115.6, 123.5, 125.2, 125.5, 126.7, 128.0, 128.4, 128.9, 129.5, 129.6, 129.7, 130.2, 131.6, 138.3, 142.6, 146.9, 157.9, 160.2, 173.6. Mass Spec (EI): *m*/*z* 468.1 ($[M]^+$ 86%), 436.1 (84), 391.1 (31), 363.1 (20), 289.1 (21), 268.1 (39), 223.1 (27), 207.1 (25), 191.1 (39), 181.0 (26), 165.1 (23), 147.0 (25), 131.0 (36), 121.0 (24), 119.0 (28), 105.0 (25), 77.0 (29), 69.1 (100). Mass Spec (HR, EI): *m*/*z* 468.1568 ($C_{29}H_{24}O_6$ requires 468.1573).

**Synthesis of Methyl 6-(Isobutyryloxy)-2-(4-(2-(isobutyryloxy)-ethoxy)phenyl))-2-phenyl-2*H*-naphtho[1,2-*b*]pyran-5-carboxylate (4).** To an ice-cooled solution of 6-hydroxy-2-(4-(2-hydroxyethoxy)phenyl)-2-phenyl-2*H*-naphtho[1,2-*b*]pyran-5-carboxylate **3** (0.2 g, 0.43 × $10^{-3}$ mol) and triethylamine (TEA) (0.36 mL, 2.57 × $10^{-3}$ mol) in dry dichloromethane ($CH_2Cl_2$) (10 mL) was added dropwise isobutyryl chloride (0.18 mL, 1.72 × $10^{-3}$ mol) under argon. The solution was stirred with ice cooling for half an hour and was then left to stir for an additional 12 h at room temperature. The solvent was evaporated under vacuum, and the residue redissolved in diethyl ether ($Et_2O$) (30 mL) and washed successively with 0.5 M HCl, water, aqueous $NaHCO_3$,

water, and brine. The organic layer was dried with $MgSO_4$ and the solvent evaporated under vacuum. The crude product was purified by column chromatography (silica gel 60, $CH_2Cl_2$), giving the product as a crunchy pink solid (200 mg, 77%). $^1$H NMR (400 MHz, $d_6$-acetone) $\delta$: 1.07−1.10 (m, 6H, 2 × $CH_3$), 1.35−1.37 (m, 6H, 2 × $CH_3$), 2.47−2.55 (m, 1H, C*H*($CH_3$)$_2$, 2.96−3.04 (m, 1H, C*H*($CH_3$)$_2$, 3.92 (br s, 3H, $COOCH_3$), 4.19−4.23 (m, 2H, $CH_2CH_2$OAr), 4.35−4.38 (m, 2H, $CH_2CH_2$OAr), 6.47 (d, *J* 10.0 Hz, 1H, pyran-CH), 6.91−6.98 (m, 3H, ArH), 7.28−7.82 (m, 10H, Ar−H), 8.45 (d, *J* 8.6 Hz, 1H, ArH). $^{13}$C NMR (100 MHz, $d_6$-acetone) $\delta$: 19.1, 19.3, 34.4, 34.7, 52.9, 63.3, 66.9, 83.6, 114.2, 115.1, 121.1, 121.8, 123.04, 123.2, 127.0, 127.3, 128.3, 128.4, 128.7, 128.8, 129.0, 129.1, 130.0, 137.8, 140.0, 145.9, 146.6, 159.3, 166.3, 175.4, 176.9.

**Synthesis of Methyl 6-(2-Bromo-2-methylpropanoyloxy)-2-(4-(2-bromo-2-methylpropanoyloxy)ethoxy)phenyl))-2-phenyl-2*H*-naphtho[1,2-*b*]pyran-5-carboxylate (7).** This compound was synthesized from **3** and 2-bromoisobutyryl bromide using the same general procedure as above and isolated as a crunchy pink solid after purification by column chromatography (silica gel 60, 1:1 $Et_2O$/hexane) (523 mg, 80%). $^1$H NMR (400 MHz, $d_6$-acetone) $\delta$: 1.86 (s, 6H, 2 × $CH_3$), 2.13 (s, 6H, 2 × $CH_3$), 3.94 (s, 3H, $COOCH_3$), 4.24−4.29 (m, 2H, $CH_2CH_2$OAr), 4.46−4.51 (m, 2H, $CH_2CH_2$OAr), 6.49 (d, *J* 10.0 Hz, 1H, pyran-CH), 6.91−7.0 (m, 3H, ArH), 7.24−7.76 (m, 9H, ArH), 8.0−8.05 (m, 1H, ArH), 8.46−8.50 (m, 1H, ArH). $^{13}$C NMR (100 MHz, $d_6$-acetone) $\delta$: 31.7, 31.9, 53.9, 57.3, 65.9, 67.4, 84.5, 115.0, 116.0, 121.8, 122.5, 123.7, 123.9, 127.8, 128.1, 128.8, 129.2, 129.8, 129.8, 129.9, 130.9, 138.6, 140.2, 146.5, 147.9, 160.0, 166.8, 171.1, 172.6.

**Synthesis of Naphthopyran 2,2-Bis(2-bromo-2-methylpropanoyloxymethyl)propionate Initiator (6).** Oxalyl chloride (579 mg, 4.60 × $10^{-3}$ mol) was added dropwise via a syringe to a solution of 2,2-bis(2-bromo-2-methylpropanoyloxymethyl)propanoic acid[19−21] (984 mg, 2.28 × $10^{-3}$ mol) in dry $CH_2Cl_2$ (10 mL), followed by one drop of DMF. The reaction was allowed to reach completion after stirring for 2.5 h at room temperature. The excess oxalyl chloride was then removed on the rotary evaporator by stripping with several portions of dichloroethane to give the corresponding acid chloride, 2,2-bis(2-bromo-2-methylpropanoyloxymethyl)propanoyl chloride, as a yellow oil that was used without further purification. The acid chloride was diluted in a small amount of dry $CH_2Cl_2$ (3 mL) and added dropwise to a solution of 6-hydroxy-2-(4-methoxyphenyl)-2-phenyl-2*H*-naphtho[1,2-*b*]pyran-5-carboxylate, **1** (906 mg, 2.07 × $10^{-3}$ mol), TEA (340 $\mu$L, 3.42 × $10^{-3}$ mol), and DMAP (13 mg, 1.06 × $10^{-4}$ mol) in dry $CH_2Cl_2$ (10 mL) at 0 °C and under argon. After stirring for 1 h at 0 °C the temperature was raised to 25 °C, and the reaction was allowed to reach completion overnight. The solvent was evaporated under vacuum, and the residue redissolved in diethyl ether ($Et_2O$) (30 mL) and washed successively with 0.5 M HCl, water, aqueous $NaHCO_3$, water, and brine. The organic layer was dried with $MgSO_4$ and the solvent evaporated under vacuum. The product was purified by column chromatography (silica gel 60, $Et_2O$/hexane) and isolated as light pink crystals (1.40 g, 80%). $^1$H NMR (400 MHz, $d_6$-acetone) $\delta$: 1.62 (s, 3H, $CH_3$), 1.98 (s, 12H, 4 × $CH_3$), 3.75 (s, 3H, Ar−$OCH_3$), 3.98 (s, 3H, $COOCH_3$), 4.62 (q, *J* 11.3 Hz, 4H, 2 × $CH_2$), 6.49 (d, *J* 10.0 Hz, 1H, pyran-CH), 6.88−6.90 (m, 2H, ArH), 6.95 (d, 1H, *J* 10.0 Hz, pyran-CH), 7.26−7.30 (m, 1H, ArH), 7.35−7.38 (m, 1H, Ar−H), 7.46−7.48 (m, 2H, Ar−H), 7.55−7.58 (m, 2H, Ar−H), 7.63−7.73 (m, 2H, Ar−H), 7.88−7.90 (m, 1H, ArH), 8.46−8.48 (m, 1H, ArH). $^{13}$C NMR (100 MHz, $d_6$-acetone) $\delta$: 19.0, 31.7, 31.7, 48.7, 54.0, 56.3, 57.8, 67.7, 84.5, 114.9, 115.2, 122.0, 122.4,123.9, 124.1, 127.7, 128.1, 128.5, 129.2, 129.7, 129.7, 129.8, 129.9, 131.0, 138.0, 139.9, 146.6, 147.9, 161.0,167.0, 172.2, 172.2.

**Synthesis of *n*-Butyl 2,2-Bis(2-bromo-2-methylpropanoyloxymethyl)propanoate (BBMPP).** This compound was synthesized from 2,2-bis(2-bromo-2-methylpropanoyloxymethyl)propanoic acid[19−21] and 1-butanol using the same general procedure as above and isolated as a clear oil after purification by column chromatography (silica gel 60, 4:1 $CH_2Cl_2$/hexane) (1 g, 67%). $^1$H NMR (400 MHz, $d_6$-acetone) $\delta$: 0.92 (t, *J* 7.4 Hz, 3H, $CH_3$), 1.35 (s, 3H, $CH_3$), 1.36−1.45 (m, 2H, $CH_2$), 1.61−1.68 (m, 2H, $CH_2$), 1.92 (s, 12H, 4 × $CH_3$), 4.15 (t, *J* 6.5 Hz, 2H, $CH_2$), 4.36 (q, *J* 11.0 Hz, 4H, 2 × $CH_2$) $^{13}$C NMR (100 MHz, (100 MHz, $d_6$-acetone) $\delta$: 13.9,18.0, 19.7, 30.9, 31.3, 47.3, 56.9, 65.6, 67.2, 171.2, 172.8, 205.9.

**General Procedure for ATRP of *n*-BA with Naphthopyran Initiator 5.** A stock solution containing *n*-BA (8.73 g, 68.10 × $10^{-3}$ mol, 5 M), naphthopyran initiator **5** (400 mg, 6.81 × $10^{-4}$ mol), and dNbpy ligand (556.5 mg, 1.36 × $10^{-3}$ mol) was prepared in benzene (3.4 g). 3 mL aliquots were added to ampules containing CuBr (22.4 mg, 1.56 × $10^{-4}$ mol); the final molar ratio of *n*-BA:**5**:ligand:CuBr was 100:1:2:1. The ampules were then degassed with three freeze−pump−thaw cycles, sealed, and then heated at 90 °C in a thermostated oil bath for 2−12.8 h. The final polymers were purified by (1) evaporation of excess monomer over a gentle stream of $N_2$, (2) dissolution of the crude mixtures into $CH_2Cl_2$, (3) precipitation into methanol, (4) decanting of supernatant liquid, (5) column chromatography (silica gel 60, 1:1 $CH_2Cl_2$/$Et_2O$) to remove residual catalyst, and (6) removal of solvent under vacuum.

**General Procedure for ATRP of *n*-BA with Naphthopyran Initiator 7.** A stock solution containing *n*-BA (9.56 g, 74.58 × $10^{-3}$ mol, 5 M), naphthopyran initiator **7** (285.8 mg, 3.73 × $10^{-4}$ mol), and dNbpy ligand (304.8 mg, 7.46 × $10^{-4}$ mol) was prepared in benzene (6.95 g). 3 mL aliquots were added to ampules containing CuBr (9.4 mg, 6.54 × $10^{-5}$ mol); the final molar ratio of *n*-BA:**7**:ligand:CuBr was 200:1:2:1. The ampules were then degassed with three freeze−pump−thaw cycles, sealed, and then heated at 90 °C in a thermostated oil bath for 1.3−5.7 h. The final polymers were purified as described above.

**General Procedure for ATRP of *n*-BA with Naphthopyran Initiator 6.** A stock solution containing *n*-butyl acrylate (8.59 g, 67.04 × $10^{-3}$ mol, 4 M), naphthopyran initiator **6** (285.8 mg, 3.35 × $10^{-4}$ mol), and dNbpy ligand (273.9 mg, 6.70 × $10^{-4}$ mol) was prepared in benzene (6.25 g). 3 mL aliquots were added to ampules containing CuBr (9.4 mg, 6.54 × $10^{-5}$ mol); the final molar ratio of *n*-BA:**6**:ligand:CuBr was 200:1:2:1. The ampules were then degassed with three freeze−pump−thaw cycles, sealed, and then heated at 90 °C in a thermostated oil bath for 1−3.5 h. The final polymers were purified as described above.

**ATRP Synthesis of p(NP)-*co*-p(BA) Copolymers 13a−13c.** A 10 mL stock solution of *n*-BA (5.65 g, 44.1 × $10^{-3}$ mol, 98 mol %), naphthopyran acrylate **11** (443 mg, 9.00 × $10^{-4}$ mol, 2 mol %), ethyl 2-bromoisobutyrate initiator (58.52 mg, 3.00 × $10^{-4}$ mol), and dNbpy ligand (245.3 mg, 6.00 × $10^{-4}$ mol) was prepared in benzene. 2.5 mL aliquots were added to ampules containing CuBr (10.8 mg, 7.50 × $10^{-5}$ mol); the final molar ratio of monomers:initiator:ligand:CuBr in each ampule was 150:1:2:1. The ampules were then degassed with three freeze−pump−thaw cycles, sealed, and then heated at 90 °C in a thermostated oil bath for 1−8.2 h. The final polymers were purified as above except column chromatography (silica gel 60) was carried out using a gradient column (DCM/hexane → DCM) to remove residual catalyst and unreacted naphthopyran monomer.

**ATRP Synthesis of p(NP)-*co*-p(BA) Copolymer 14a.** A stock solution of *n*-BA (2.25 g, 17.6 × $10^{-3}$ mol, 99 mol %), naphthopyran methacrylate **12** (90 mg, 1.78 × $10^{-4}$ mol, 1 mol %), BBMPP initiator (64.25 mg, 1.32 × $10^{-4}$ mol), and dNbpy ligand (107.6 mg, 2.63 × $10^{-4}$ mol) was prepared in benzene (1.25 g). This solution was transferred to an ampule containing CuBr (18.9 mg, 1.32 × $10^{-4}$ mol); the final molar ratio of monomers:initiator:ligand:CuBr in each ampule was 135:1:2:1. The ampules were then degassed with three freeze−pump−thaw cycles, sealed, and then heated at 90 °C in a thermostated oil bath for 2 h. The final polymer was purified by (1) evaporation

of excess monomer over a gentle stream of $N_2$, (2) dissolution of the crude mixtures into $CH_2Cl_2$, (3) precipitation into methanol, (4) decanting of supernatant liquid, (5) column chromatography (silica gel 60, 1:1 $CH_2Cl_2/Et_2O$) to remove residual catalyst, and (6) removal of solvent under vacuum.

**ATRP Synthesis of Triblock Copolymer 15a, NP-[p(*n*-BA)$_{25}$-*b*-p(IBA)$_{54}$]$_2$.** A stock solution containing *n*-BA (1.55 g, 12.08 $\times$ $10^{-3}$ mol, 4 M), naphthopyran initiator **6** (103 mg, 1.21 $\times$ $10^{-4}$ mol), and dNbpy ligand (98.7 mg, 2.42 $\times$ $10^{-4}$ mol) was prepared in benzene (1.13 g) and added to an ampule containing CuBr (17.3 mg, 1.21 $\times$ $10^{-4}$ mol); the final molar ratio of *n*-BA:**6**:ligand:CuBr was 100:1:2:1. The ampule was degassed with three freeze−pump−thaw cycles, sealed, and then heated at 90 °C in a thermostated oil bath for 1 h. The final polymer was purified by (1) evaporation of excess monomer over a gentle stream of $N_2$, (2) dissolution of the crude mixtures into $CH_2Cl_2$, (3) precipitation into methanol, (4) decanting of supernatant liquid, (5) column chromatography (silica gel 60, 1:1 $CH_2Cl_2/Et_2O$) to remove residual catalyst, and (6) removal of solvent under vacuum. Block extension was carried out by making a solution of the purified p(*n*-BA) macroinitiator (654 mg, 9.16 $\times$ $10^{-5}$ mol), IBA (2.86 g, 13.74 $\times$ $10^{-3}$ mol, 3.2 M), and dNbpy ligand (74.9 mg, 1.83 $\times$ $10^{-4}$ mol) in benzene (1.22 g) and adding this to an ampule containing CuBr (13.1 mg, 9.16 $\times$ $10^{-5}$ mol); the final molar ratio of [monomer]/[CuBr]/[4,4′-dinonyl-2,2′-bipyridine]/[macroinitiator] = 154:1:2:1. The ampule was then degassed with three freeze−pump−thaw cycles, sealed, and then heated at 90 °C in a thermostated oil bath for 4 h 10 min. The final polymers were purified by (1) dissolution of the crude mixtures into $CH_2Cl_2$, (2) precipitation into methanol, (3) decanting of supernatant liquid, (4) column chromatography (silica gel 60, 1:1 $CH_2Cl_2/Et_2O$) to remove residual catalyst, and (5) removal of solvent under vacuum.

**ATRP Synthesis of Triblock Copolymer 15b, NP-[p(*n*-BA)$_{35}$-*b*-p(IBA)$_{65}$]$_2$.** A stock solution containing *n*-BA (4.03 g, 31.40 $\times$ $10^{-3}$ mol, 4 M), naphthopyran initiator **6** (134 mg, 1.57 $\times$ $10^{-4}$ mol), and dNbpy ligand (128 mg, 3.14 $\times$ $10^{-4}$ mol) was prepared in benzene (2.93 g). A 3 g aliquot was added to an ampule containing CuBr (9.37 mg, 6.53 $\times$ $10^{-5}$ mol); the final molar ratio of *n*-BA:**6**:ligand:CuBr was 200:1:2:1. The ampule was degassed with three freeze−pump−thaw cycles, sealed, and then heated at 90 °C in a thermostated oil bath for 1 h 20 min. The final polymer was purified by (1) evaporation of excess monomer over a gentle stream of $N_2$, (2) dissolution of the crude mixtures into $CH_2Cl_2$, (3) precipitation into methanol, (4) decanting of supernatant liquid, (5) column chromatography (silica gel 60, 1:1 $CH_2Cl_2/Et_2O$) to remove residual catalyst, and (6) removal of solvent under vacuum. Block extension was carried out by making a solution of the purified p(*n*-BA) macroinitiator (460 mg, 4.76 $\times$ $10^{-5}$ mol), IBA (1.49 g, 7.14 $\times$ $10^{-3}$ mol, 3.2 M), and dNbpy ligand (38.9 mg, 9.52 $\times$ $10^{-5}$ mol) in benzene (0.63 g) and adding this to an ampule containing CuBr (6.83 mg, 4.76 $\times$ $10^{-5}$ mol); the final molar ratio of [monomer]/[CuBr]/[4,4′-dinonyl-2,2′-bipyridine]/[macroinitiator] = 150:1:2:1. The ampule was then degassed with three freeze−pump−thaw cycles, sealed, and then heated at 90 °C in a thermostated oil bath for 4 h 10 min. The final polymers were purified by (1) dissolution of the crude mixtures into $CH_2Cl_2$, (2) precipitation into methanol, (3) decanting of supernatant liquid, (4) column chromatography (silica gel 60, 1:1 $CH_2Cl_2/Et_2O$) to remove residual catalyst, and (5) removal of solvent under vacuum.

**ATRP Synthesis of Triblock Copolymer 15c, NP-[p(*n*-BA)$_{60}$-*b*-p(IBA)$_{30}$]$_2$.** A stock solution containing *n*-butyl acrylate (4.03 g, 31.40 $\times$ $10^{-3}$ mol, 4 M), naphthopyran initiator **6** (134 mg, 1.57 $\times$ $10^{-4}$ mol), and dNbpy ligand (128 mg, 3.14 $\times$ $10^{-4}$ mol) was prepared in benzene (2.93 g). A 3 g aliquot was added to an ampule containing CuBr (9.37 mg, 6.53 $\times$ $10^{-5}$ mol); the final molar ratio of *n*-BA:**6**:ligand:CuBr was 200:1:2:1. The ampule was degassed with three freeze−pump−thaw cycles, sealed, and then heated at 90 °C in a thermostated oil bath for 2 h 50 min. The final polymer was purified by (1) evaporation of excess monomer over a gentle stream of $N_2$, (2) dissolution of the crude mixtures into $CH_2Cl_2$, (3) precipitation into methanol, (4) decanting of supernatant liquid, (5) column chromatography (silica gel 60, 1:1 $CH_2Cl_2/Et_2O$) to remove residual catalyst, and (6) removal of solvent under vacuum. Block extension was carried out by making a solution of the purified p(*n*-BA) macroinitiator (672 mg, 4.10 $\times$ $10^{-5}$ mol), IBA (1.28 g, 6.15 $\times$ $10^{-3}$ mol, 3.2 M), and dNbpy ligand (33.5 mg, 8.20 $\times$ $10^{-5}$ mol) in benzene (0.85 g) and adding this to an ampule containing CuBr (5.88 mg, 4.10 $\times$ $10^{-5}$ mol); the final molar ratio of [monomer]/[CuBr]/[4,4′-dinonyl-2,2′-bipyridine]/[macroinitiator] = 144:1:2:1. The ampule was then degassed with three freeze−pump−thaw cycles, sealed, and then heated at 90 °C in a thermostated oil bath for 4 h 10 min. The final polymers were purified by (1) dissolution of the crude mixtures into $CH_2Cl_2$, (2) precipitation into methanol, (3) decanting of supernatant liquid, (4) column chromatography (silica gel 60, 1:1 $CH_2Cl_2/Et_2O$) to remove residual catalyst, and (5) removal of solvent under vacuum.

**ATRP Synthesis of Triblock Copolymer 16a, (*n*-butyl)-[(p-(NP)$_{0.01}$-*co*-p(*n*-BA)$_{0.99}$)$_{58}$-*b*-p(IBA)$_{28}$]$_2$.** A solution of macroinitiator **14a** (681 mg, 3.98 $\times$ $10^{-5}$ mol), IBA (1.24 g, 5.97 $\times$ $10^{-3}$ mol, 3.2 M), and dNbpy ligand (32.51 mg, 7.96 $\times$ $10^{-5}$ mol) in benzene (0.53 g) was added to an ampule containing CuBr (5.71 mg, 3.98 $\times$ $10^{-5}$ mol); the final molar ratio of [monomer]/[CuBr]/[4,4′-dinonyl-2,2′-bipyridine]/[macroinitiator] = 150:1:2:1. The ampule was then degassed with three freeze−pump−thaw cycles, sealed, and then heated at 90 °C in a thermostated oil bath for 4 h 10 min. The final polymers were purified by (1) dissolution of the crude mixtures into $CH_2Cl_2$, (2) precipitation into methanol, (3) decanting of supernatant liquid, (4) column chromatography (silica gel 60, 1:1 $CH_2Cl_2/Et_2O$) to remove residual catalyst, and (5) removal of solvent under vacuum.

**Preparation of Photochromic Lens Samples.** The naphthopyran−p(*n*-BA) conjugates (or controls) were individually dissolved in a standard industrial lens formulation made up of 1:4 weight ratio of poly(ethylene glycol) (400) dimethacrylate and 2,2′-bis((4-methacryloxyethoxy)phenyl)propane (specific monomer structures given below) with 0.4 mass % AIBN. The samples were then cured at 80 °C for 16 h in a mold to give optically clear test samples of equivalent thickness (~2.4 mm). They were each doped at equivalent concentrations of 1.5 $\times$ $10^{-7}$ mol of photochromic-polymer conjugate per gram of lens formulation. This concentration was chosen in order to maintain optical densities in a meaningful detector range for photochromic kinetic tests.

**Preparation of Photochromic Films.** Block copolymers were dissolved in toluene (3 M) and then cast onto glass slides. The films were left to dry at room temperature for 8 h and then dried in a vacuum oven at 100 °C overnight.

**Acknowledgment.** F.E. thanks the CRC for Polymers for funding the research in association with CAMD, School of Chem. Eng. and Ind. Chem., UNSW and CSIRO Molecular and Health Technologies for providing laboratory space. F.E. also acknowledges the assistance of Dr. Jonathan Campbell (UNSW) for the setup and maintenance of photochromic testing equipment. T.P.D. acknowledges the receipt of a Federation fellowship from the ARC.

**Supporting Information Available:** Example $^1$H NMR spectra of naphthopyran−polymer conjugates and photochromic initiators, polymerization kinetic plots, and GPC traces. This material is available free of charge via the Internet at http://pubs.acs.org.

## References and Notes

(1) Higgins, S. *Chem. Br.* **2003**, *26*, 26–29.

(2) Van Gemert, B. In *Organic Photochromic and Thermochromic Compounds*; Crano, J., Guglielmetti, R., Eds.; Plenum Publishing: New York, 1998; Vol. *1*, Chapter 3, p 111–137.
(3) Delbaere, S.; Micheau, J.-C.; Vermeersch, G. *J. Org. Chem.* **2003**, *68*, 8968–8973.
(4) Delbaere, S.; Luccioni-Huoze, B.; Bochu, C.; Teral, Y.; Campredon, M.; Vermeersch, G. *J. Chem. Soc., Perkin Trans. 2.* **1998**, 1153–1157.
(5) Naour-Sene, L. L. Process of intergrating a photochromic substance into an opthalmic lens and a photochromic lens of organic material. US 4,286,957, **1981**.
(6) Maltman, W. R.; Threlfall, I. M. Process for manufacturing photochromic articles. US 4,851,471, **1989**.
(7) Krongauz, V. *Environmental Effects on Organic Photochromic Systems*, 1st ed.; Dürr, H.; Bouas-Laurent, H., Eds.; Elsevier House Publishing House: Amsterdam: 1990; Vol. 40, pp 793−820.
(8) Evans, R. A.; Such, G. K.; Malic, N.; Davis, T. P.; Lewis, D. A.; Campbell, J. A. Photochromic Compounds Comprising Polymeric Substituents and Methods for Preparation and Use Thereof. WO2006024099, **2006**.
(9) Evans, R. A.; Hanley, T. L.; Skidmore, M. A.; Davis, T. P.; Such, G. K.; Yee, L. H.; Ball, G. E.; Lewis, D. A. *Nat. Mater.* **2005**, *4*, 249–254.
(10) Ercole, F.; Davis, T. P.; Evans, R. A. *Macromolecules* **2009**, *42*, 1500–1511.
(11) Such, G. K.; Evans, R. A.; Davis, T. P. *Macromolecules* **2004**, *37*, 9664–9666.
(12) Such, G. K.; Evans, R. A.; Davis, T. P. *Mol. Cryst. Liq. Cryst.* **2005**, *430*, 273–279.
(13) Such, G. K.; Evans, R. A.; Davis, T. P. *Macromolecules* **2006**, *39*, 1392–1396.
(14) Malic, N.; Campbell, J. A.; Evans, R. A. *Macromolecules* **2008**, *41*, 1206–1214.
(15) Malic, N.; Evans, R. A. *Aust. J. Chem.* **2006**, *59*, 763–771.
(16) Kumar, A.; VanGemert, B.; Knowles, D. B. Novel substituted naphthopyrans. WO 95/16215, **1995**.
(17) Ercole, F.; Malic, N.; Davis, T. P.; Evans, R. A. *J. Mater. Chem.* **2009**, *19*, 5612–5623.
(18) Ihre, H.; Hult, A.; Soderlind, E. *J. Am. Chem. Soc.* **1996**, *118*, 6388–6395.
(19) Shi, Y.; Fu, Z.; Li, B.; Zhang, L.; Cai, X.; Zhang, D. *Eur. Polym. J.* **2007**, *43*, 2612–2619.
(20) Liu, Q.; Zhao, P.; Chen, Y. *J. Polym. Sci., Part A: Polym. Chem.* **2007**, *45*, 3330–3341.
(21) Heise, A.; Nguyen, C.; Malek, R.; Hedrick, J. L.; Frank, C. W.; Miller, R. D. *Macromolecules* **2000**, *33*, 2346–2354.
(22) Postma, A.; Davis, T. P.; Li, G. X.; Moad, G.; O′Shea, M. S. *Macromolecules* **2006**, *39*, 5307–5318.
(23) Hakim, M.; Verhoeven, V.; McManus, N. T.; Dube′, M. A.; Penlidis, A. *J. App. Polym. Sci.* **2000**, *77* (3), 602–609.
(24) Biteau, J.; Chaput, F.; Boilot, J. *J. Phys. Chem.* **1996**, *100*, 9024–9031.
(25) Such, G. K.; Evans, R. A.; Davis, T. P. *Macromolecules* **2006**, *39*, 9562–9570.
(26) Sriprom, W.; Néel, M.; Gabbutt, C. D.; Heron, M.; Perrier, S. *J. Mater. Chem.* **2007**, *17*, 1885–1893.
(27) Dervaux, B.; Van Camp, W.; Van Renterghem, L.; Du Prez, F. E. *J. Polym. Sci., Part A: Polym. Chem.* **2008**, *46*, 1649–1661.
(28) Beuermann, S.; Paquet, D. A., Jr.; Mc Minn, J. H.; Hutchinson, R. A. *Macromolecules* **1996**, *29*, 4206–4215.